5-1-2012

Effects of Hyperthermia on Photochemical Internalization-mediated Delivery of Bleomycin

Christina Schlazer
University of Nevada, Las Vegas

Follow this and additional works at: https://digitalscholarship.unlv.edu/thesesdissertations

Part of the Neurology Commons, Neurosciences Commons, Oncology Commons, and the Physics Commons

EFFECTS OF HYPERTHERMIA ON PHOTOCHEMICAL INTERNALIZATION-

MEDIATED DELIVERY OF BLEOMYCIN

By

Christina Schlazer

Bachelor of Science in Physics
Bachelor of Arts in Mathematical Science
Binghamton University
2006

A thesis submitted in partial fulfillment
of the requirements for the

Master of Science Degree in Health Physics

Department of Health Physics and Diagnostic Sciences
Division of Health Sciences
The Graduate College

University of Nevada, Las Vegas
May 2012

THE GRADUATE COLLEGE

We recommend the thesis prepared under our supervision by

Christina Schlazer

entitled

Effects of Hyperthermia on Photochemical Internalization-Mediated Delivery of Bleomycin

be accepted in partial fulfillment of the requirements for the degree of

Master of Science in Health Physics
Department of Health Physics and Diagnostic Sciences

Steen Madsen, Ph.D., Committee Chair

Ralf Sudowe, Ph.D., Committee Member

Gary Cerefice, Ph.D., Committee Member

Janet Dufek, Ph.D., Graduate College Representative

Ronald Smith, Ph. D., Vice President for Research and Graduate Studies
and Dean of the Graduate College

May 2012

ABSTRACT

Standard treatment protocols for high-grade gliomas, such as glioblastoma multiforme (GBM), are highly ineffective due to their inability to eradicate infiltrating tumor cells. Improvements in overall survival are likely to be realized only with the development of more effective localized therapies capable of eradicating tumor cells in the surgical resection margin and beyond. Photochemical internalization (PCI) is a localized light-based therapeutic modality that enhances the efficacy of therapeutic macromolecules including chemotherapeutic agents such as bleomycin. A number of studies have shown that this photodynamic therapy (PDT) - based modality may prove effective in the treatment of high-grade gliomas.

Three-dimensional multicell human glioma spheroids were used as a tumor model to investigate the efficacy of combination therapies consisting of hyperthermia and PCI. Hyperthermia has been shown to increase the efficacy of a number of therapies including radiation and chemotherapy, however, there have been no studies investigating its utility in combination with PCI.

The results show that hyperthermia and PCI interact in a synergistic manner over a very narrow range of light and temperature levels. In this tumor model, temperatures of 45 $^{\circ}$C resulted in total spheroid death: the exact hyperthermic threshold was estimated to be between 42 and 45 $^{\circ}$C which provided the rationale for the temperature range investigated (40 – 42 $^{\circ}$C). No significant differences in growth kinetics and survival were observed between PCI- and PDT -exposed spheroids at radiant exposures < 1.5 J cm^{-2}. In

contrast, all PDT and PCI spheroids irradiated with 3.0 J cm^{-2} died, suggesting that the useful light range is between 1.5 and 3.0 J cm^{-2}.

A relatively low level of synergism was observed between PCI and hyperthermia at 1.5 J cm^{-2} and 40 $^{\circ}$C, while a high degree of synergism was found when the two modalities were combined at a light level of 2.5 J cm^{-2} and a temperature of 42 $^{\circ}$C. This is the first observation of a synergistic interaction between PCI and hyperthermia and, collectively, the results provide the rationale for additional studies in animal brain tumor models.

ACKNOWLEDGMENTS

This research project would not have been realized without the gracious support of so many people. I would first like to thank my advisor, Dr. Steen Madsen, he always gave me guidance and excellent advice during my study and research here at UNLV.

I wish to extend my thanks to the thesis committee members, Dr. Ralf Sudowe, Dr. Janet Dufek, and Dr. Gary Cerefice. I am honored to have this group of scientists in my committee.

Special thanks are also in order for the wonderful support of Van Vo, Mary Turner, and Doris Coomes during the course of my research and studies at UNLV.

I would finally like to express my gratitude to all my friends and family. Thank you to my parents, for all your support and encouragement over the years. I'd especially like to thank my husband, Mike, for always supporting me after a long day in the laboratory.

TABLE OF CONTENTS

LIST OF FIGURES

CHAPTER 1

INTRODUCTION

1.1 Malignant Brain Tumors

Primary malignant brain tumors are uncommon and represent 2 percent of all adult cancers in the United States [Iacob 2009]. Gliomas are a non-uniform group of tumors in the central nervous system (CNS). They can be classified as astrocytomas, ependymomas, and oligodendrogliomas. Astrocytomas are the most common and are classified as low-grade, while anaplastic astrocytomas and glioblastomas are considered grades III and IV, respectively [Iacob 2009]. The most common type is glioblastoma multiforme (GBM) which has a dismal prognosis. Although a number of causes have been suggested (electromagnetic fields, cellular phones, head trauma, pesticides, N-nitroso compounds in food products such as cheese and fish, and genetic syndromes), the only proven risk factor for the development of GBM is exposure to high dose ionizing radiation [Chandana 2008]. Common symptoms include nausea, vomiting, headaches, seizures, personality changes, and neurocognitive deficit. The American Cancer Society estimates there are 12,000 deaths per year in the United States due to brain and nervous system cancers. As shown in Figure 1, the occurrence of primary brain tumors is highest between the ages of 65 and 79 years with a slightly higher frequency in men [Chandana 2008].
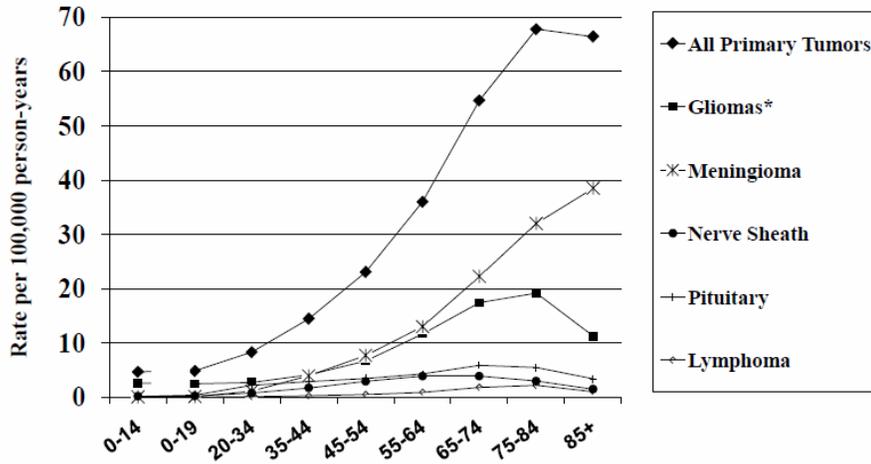
Figure 1. Age-Specific Incidence of Primary Brain and CNS Tumors by Selected Histologies; collected 2004-2007. (Adapted from CBTRUS 2011)

Of the estimated 51,000 primary brain tumors diagnosed in the United States every year, 36 percent are gliomas. Approximately 50% of gliomas are GBM (Figure 2) [Clarke 2010].
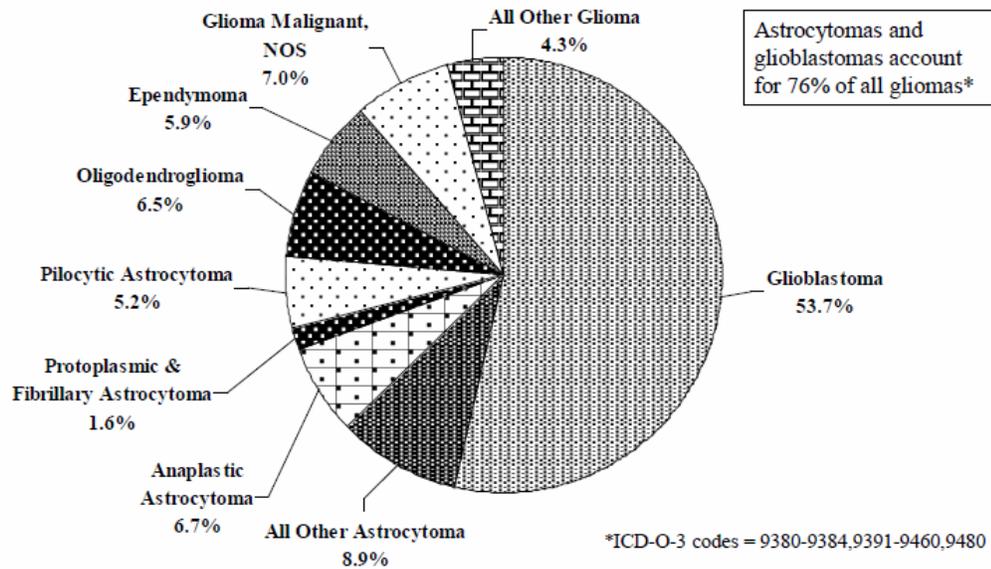
Figure 2. Distribution of all primary brain and CNS gliomas by histology subtypes; collected 2004-2007. (Adapted from CBTRUS 2011)

1.2 Glioblastoma

Starting in 2005, the standard treatment therapy for GBM consists of surgical resection followed by chemotherapy with temozolomide and radiation up to 60 Gy. Temozolomide (TMZ) is an alkylating agent that attaches an alkyl group to DNA resulting in irreparable damage. The median survival for patients receiving this treatment regimen is 14.6 months compared to 12.1 months for patients treated with radiation only [Pan 2011]. Even with the combined treatments, the disease almost always recurs [Nishikawa 2010]. In many cases, the complete removal of a glioma is not possible due to extensive tumor cell infiltration into normal brain. The aim of current treatment regimens is to eliminate these infiltrative cells [Iacob 2009].

Diagnosing a brain tumor starts with imaging, followed by histopathology to verify the diagnosis. Recent advances in brain imaging techniques have resulted in improved tumor localization and evaluation of functional status. Imaging is also commonly used to determine treatment outcome. Gadolinium-enhanced magnetic resonance imaging (MRI) is the recommended method for the initial anatomic assessment of brain lesions. MRI is preferred to computed tomography because of its superior soft tissue contrast which allows for more accurate assessments of lesions in the spine, brainstem, and cerebellum. Magnetic resonance spectroscopy can also be used to provide metabolic and biochemical information about the tumor. By pinpointing the cortical regions that control language, memory, and motor functions, functional MRI can be used for neurosurgical planning and neurologic risk evaluation. Positron emission tomography (PET) is an important tool for evaluating the aggressiveness of the tumor and locating highly metabolic areas within the tumor. PET can also be used during the follow-up

phase to evaluate the efficacy of treatment and to delineate tumor recurrence from radiation-induced necrosis.

A biopsy of the tumor tissue will determine the diagnosis and the type of treatment required. The choice to perform complete tumor resection depends on the location of the tumor. Complete resection is possible for some tumor types, however, the situation is complicated for high-grade gliomas such as GBM since tumor cells tend to migrate into the normal brain where they cannot be detected with current clinical imaging modalities. Since these cells are responsible for tumor recurrence, efforts must be devoted to find therapeutic approaches to eradicate these highly infiltrative cells. To that end, a number of local therapies, including photodynamic therapy (PDT) and photochemical internalization (PCI) have been proposed.

After surgery, the standard treatment of high grade gliomas calls for external or internal radiation including highly conformal techniques such as stereotactic radio-surgery. Despite significant advances in radiation delivery devices, allowing for highly conformal treatments (and dose escalation), high-dose radiotherapy has had minimal impact on overall survival. This is probably due to the infiltrative nature of glioma cells, i.e., many of these cells have migrated into normal brain where the radiation dose is insufficient to eradicate them and hence, they form the locus of new tumors.

Delivery of drugs to the brain is complicated by the presence of the blood-brain barrier (BBB) which prevents most therapeutic agents (including chemotherapeutic compounds) from entering the brain. This poses a significant challenge for the eradication of infiltrating tumor cells. A number of different delivery methods have been attempted in order to address the difficulties posed by the BBB. For example, drug-

containing wafers have been placed in the surgical cavity after tumor removal and used in combination with radiation therapy. Convection-enhanced delivery (CED) approaches have also been attempted. Typically, CED uses multiple catheters implanted in the resection cavity following tumor removal. The chemotherapeutic agent is introduced into the resection cavity and brain adjacent to tumor via positive pressure infusion [Clarke 2010]. The recent introduction of the chemotherapeutic agent, temozolomide, represents a significant development in the treatment of GBM since this drug has been shown to prolong overall survival by 2-3 months [Fadul 2008]. Due to its small molecular weight, TMZ efficiently crosses the BBB without significant adverse effects [Koukourakis 2009].

Due to the lack of efficacy of current GBM treatments, a wide variety of investigational therapies are currently being evaluated in both pre-clinical and clinical studies. For example, PDT is a localized laser-based treatment approach that has shown promise for the eradication of infiltrating glioma cells within a few cm of the resection margin [Mathews 2009].

1.3 Photodynamic Therapy

PDT is based, in part, on the observation that photosensitizers show preferential accumulation in tumor cells. Light absorption at resonant wavelengths results in photosensitizer excitation and subsequent cytotoxicity. Cytotoxicity is predominantly caused by a singlet oxygen-mediated reaction that causes damage to enzymes, plasma membranes, and cytoplasmic or nuclear organelles. PDT dosimetry is complex as it depends on a number of parameters including photosensitizer concentration, light dose, dose rate, and oxygen concentration [Dubessy 2000]. A threshold dose is required in

order to induce cytotoxicity and this may be difficult to achieve *in vivo* due to a number of factors including limited light penetration in biological tissues and inadequate oxygen and photosensitizer concentrations in tumor tissues [Hogset 2004].

PDT is initiated with the absorption of light by a photosensitizer which results in a transition to an electronically excited singlet state (Figure 3) [Berg 2005]. De-excitation to the ground state occurs with high probability and results in prompt emission of fluorescence. De-excitation to a triplet state via inter-system crossing occurs with low probability. The triplet photosensitizer can de-excite via type I or II mechanisms (Figure 4). For the vast majority of photosensitizers, deactivation occurs primarily via a type II mechanism in which the excited triplet state sensitizer interacts with ground state triplet molecular oxygen resulting in the generation of singlet molecular oxygen – a strong oxidizing agent capable of causing significant damage to amino acids, unsaturated fatty acids, cholesterol, and guanine [Berg 2005].
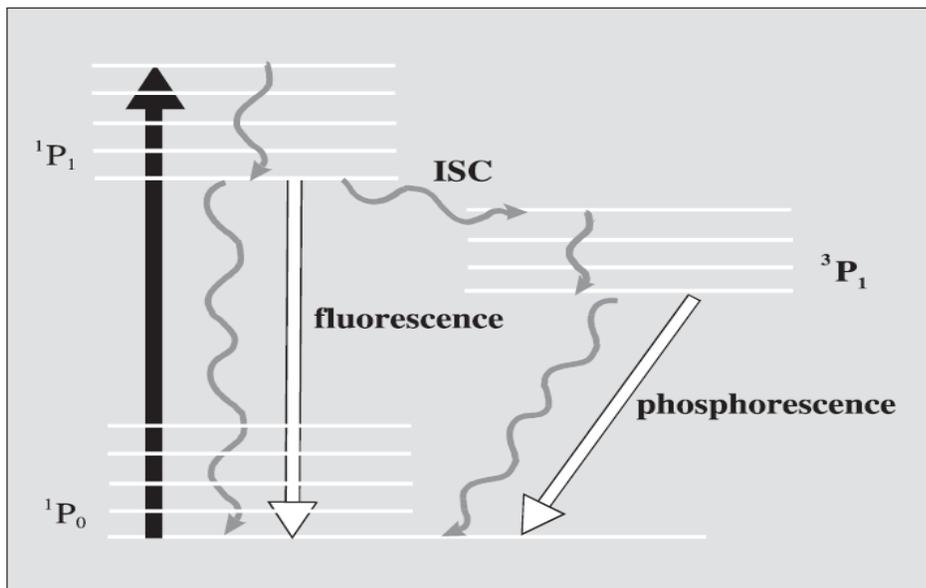
Figure 3. Jablonski diagram showing electronic states following absorption of light by a photosensitizer [Berg 2005].
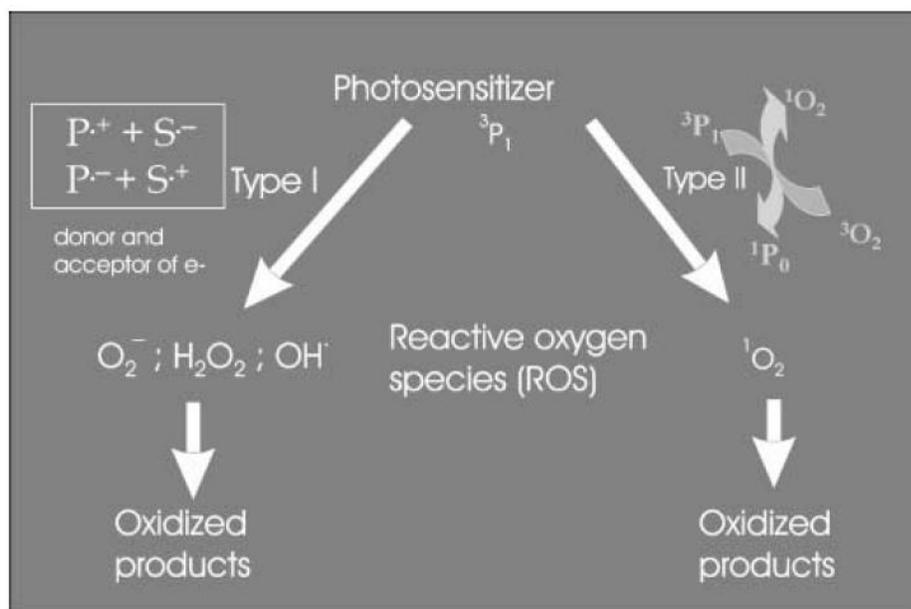
Figure 4. Photochemical reaction pathways from the triplet state of a photosensitizer [Berg 2005].

Since singlet oxygen has a range of < 20 nm, the intended target must be close to the excited photosensitizer in order to be affected [Hogset 2004]. A good photosensitizer should have a high probability of triplet formation and the triplet state should be long-lived in order to react with neighboring molecules [Berg 2005]. Depending on the photosensitizer and cell line, the photodynamic effects will lead to apoptosis, necrosis, or autophagy [Gupta 2010].

1.4 Photochemical Internalization

PCI is designed to improve the use of macromolecules in cancer therapy in a site-specific manner [Dietze 2005]. The technique is summarized in Figures 5 and 6. PCI is a special version of PDT in which a plasma membrane localizing photosensitizer

and a macromolecule (e.g. bleomycin) is localized in endocytic vesicles of target cells (e.g. infiltrating glioma cells).
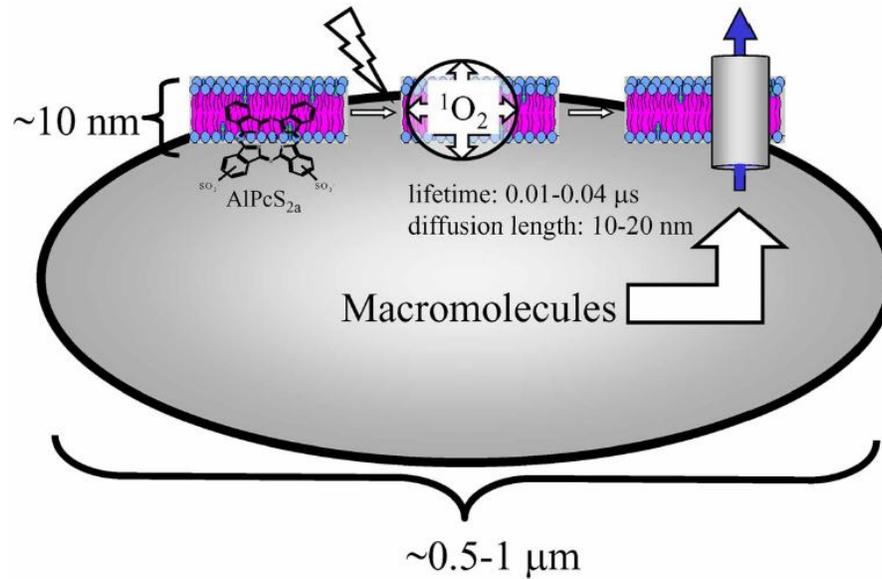
Figure 5. An endocytic vesicle containing a photosensitizer and macromolecule undergoing PCI. When light is incident on the vesicle, reactive oxygen species are formed, the membrane is broken and the macromolecule is released into the cytosol, but only in the irradiated area [Hogset 2004].
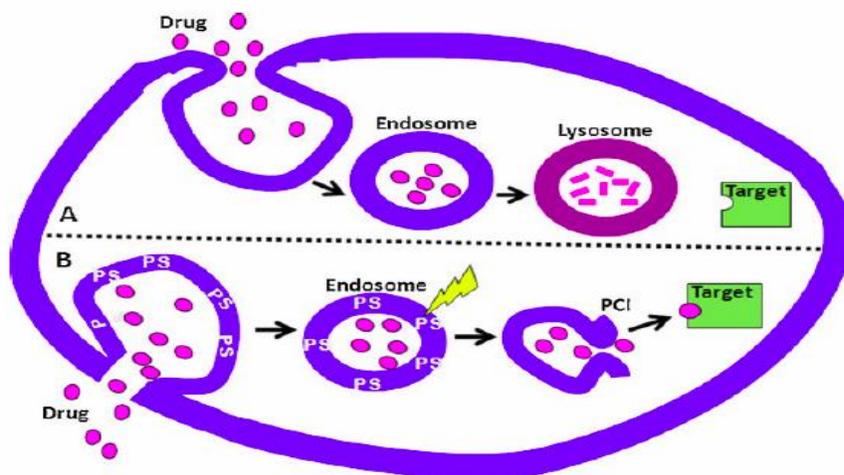
Figure 6. Illustration of PCI. A: Drugs enter cells via endocytosis and are transported to lysosomes where they are eventually degraded before serving their function. B: Photosensitizer accumulates on endosome membranes and light exposure causes the membrane to rupture thus releasing the drug into the cytosol where it is free to diffuse to the target [Weyergang 2011].

Photosensitizers used in PCI must have a strong affinity for the plasma membrane. Such compounds will be incorporated into the membranes of endosomes and, following light activation, will result in the disruption of the membrane and subsequent release of the contents of the endosome. The photosensitizer must be excluded from the endosome interior in order to prevent damage to the contents of the endosome [Hogset 2004].

Aluminum phthalocyanine disulfonate ($AlPcS_{2a}$) is the most common photosensitizer used in PCI (Figure 7). Photosensitizers are characterized by their structure. The efficiency and localization within the cell depends on how their polar and hydrophobic chains are distributed.
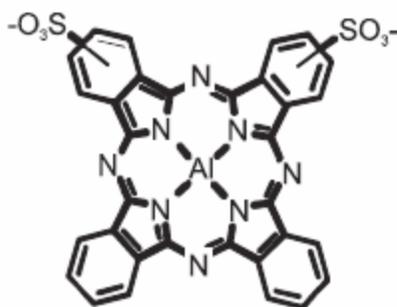
Figure 7. The chemical structure of aluminum phthalocyanine disulfonate (AlPcS$_{2a}$) with two sulfonate groups on adjacent rings [Hogset 2004].

AlPcS$_{2a}$ is a second generation amphiphilic photosensitizer with both hydrophilic and lipophilic domains [Bonneau 2004] and, as such, has excellent membrane penetrating properties, and high phototoxicity [Peng 1990]. Sulphonated aluminum phthalocyanine sensitizers are useful in PDT because of their stronger absorption at longer wavelengths of 650-800 nm [Ambroz 1990] where light penetration in biological tissues is optimal. Typically, the 670 nm absorption resonance is used in PCI applications. Additionally, AlPcS$_{2a}$ has low absorption at other wavelengths, thus reducing the potential for skin photosensitivity [Gupta 2010].

The rapid attenuation of light in most tissues, including the brain, should lead to minimal side effects since the effect is localized to the irradiated area. The endosomal escape of macromolecules including genes, oligonucleotides and proteins by means of PCI has been documented both *in vitro* and *in vivo* and has been shown to increase the therapeutic effect in a synergistic manner [Dietze 2005, Selbo 2000]. Compared to other drugs, macromolecules (e.g. nucleic acids, peptides, proteins, and synthetic polymers) are

very specific when it comes to targeting [Hogset 2004]. The delivery of these macromolecules to targets within the cell is often problematic since their associated delivery vehicle (the endosome) is often degraded in lysosomes. Therefore, the macromolecules are often destroyed prior to reaching their target (e.g. the DNA in the nucleus). PCI solves this problem by releasing the macromolecules from the endosome prior to lysosomal degradation [Berg 2007].

One benefit of using PCI is that there are no size restrictions for the delivery of molecules, such as chemotherapeutic agents [Hogset 2004]. PCI releases drugs that normally would be degraded in lysosomes thereby increasing the efficacy of the agent. Consequently, lower doses may be used thus minimizing the probability of adverse effects to the patient [Weyergang 2011]. PCI is limited by the penetration depth of light in biological tissues. For example, the penetration depth (e^{-1} intensity) of 670 nm light in brain tissues is approximately 2 mm. However, the low light fluences required for the PCI effect suggest that treatment depths of 1-2 cm should be possible [Hogset 2004]. This is significant since the majority of GBM tumors recur within 2 cm of the resection cavity [Wallner 1989].

1.5 Bleomycin

Bleomycin (BLM) is a 1.5 kDa glycopeptic antibiotic that has been used in a number of chemotherapeutic regimens for the treatment of a variety of cancers including, squamous cell carcinomas of the head and neck, esophagus, bronchus, and skin, as well as Hodgkin's and non-Hodgkin's lymphoma [Dietze 2005]. BLM is water-soluble and was discovered in 1966 by Hamao Umezawa [Umezawa 1966]. BLM was originally

used as copper complexes from streptomyces verticillus [Roy 1984]. BLM has been used in brain tumor treatments since the early 1970's and is delivered directly to the tumor since it does not pass through the intact BBB [Linnert 2009]. BLM is a mixture of eleven molecules that differ in their terminal amine part, which is involved in nucleic acid interactions. BLM also has a glycannic part, a bithiazole moiety that binds to the DNA, and a pseudopeptidic area that binds transition metals and is used in sequence recognition (Figure 8) [Mir 1996].

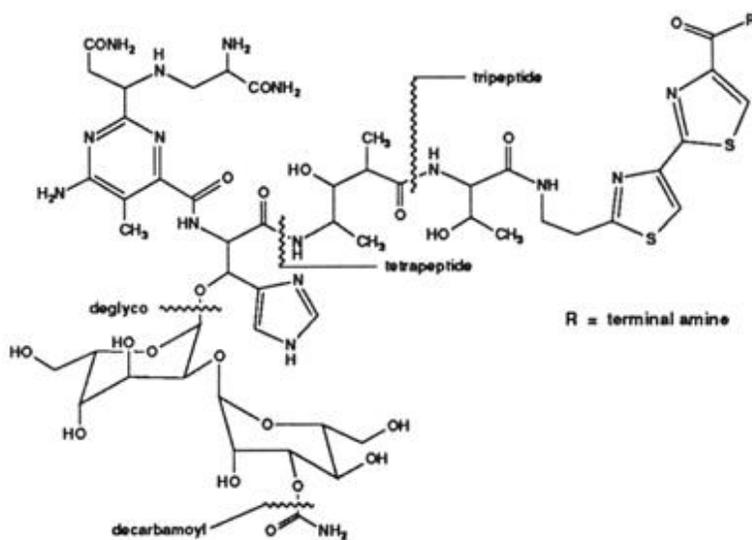**Figure 8.** The structure of bleomycin [Stubbe 1986].

The molecule exerts its toxic effects by causing single and double-strand DNA breaks [Zaniboni 2005, Roy 1984]. Bleomycin induces single-strand and double-strand DNA breaks with a 10:1 ratio resulting in cell arrest in the G2-M phase. In order to create these effects, BLM must pass through the cellular membrane and diffuse to the nucleus [Stubbe 1986].

BLM has a high intrinsic cytotoxicity, but since it cannot diffuse through the cell membrane, its capabilities are limited [Mir 1996]. Due to the limited penetration of BLM through the plasma membrane, tumor cells have a relatively low sensitivity to this anti-cancer agent. BLM enters cells via receptor-mediated endocytosis resulting in its encapsulation in endosomes. Once in the cytosol, most endosomes end up in the lysosomes along with their contents (bleomycin). Therefore, the vast majority of BLM never reaches the DNA [Pron 1999]. Due to its poor efficacy, BLM is typically used in combination with other agents [Mir 1996].

1.6 Hyperthermia

As a therapeutic procedure, hyperthermia produces elevated tissue temperatures resulting in impairment of cellular function. Specifically, increased temperatures affect enzymatic and structural function within the cells. This can affect cell growth, and lead to cell death via apoptosis and necrosis, depending on the temperature [Van der Zee 2002]. Hyperthermia causes changes in the cell membrane that can reduce transmembrane transport and destabilize the cell's potential [Dereski 1995]. Additionally, hyperthermia can result in inhibition of nucleic acid synthesis, and enzyme repair, and changes in DNA conformality [Van der Zee 2002]. From a therapeutic perspective, tumor cells are less resistant to sudden increases in temperature than normal cells.

Temperature increases can be achieved by different techniques including microwaves, radiofrequency, ultrasound, or electrically-induced methods. All of these approaches have yielded good results, but there is still the problem of obtaining

13

homogeneous temperature distributions throughout large tumors. Failure to achieve adequate temperature elevations throughout the tumor results in recurrence, whereas overheating can result in undesirable inflammatory responses [Silva 2011]. Superficial tumors are excellent candidates for hyperthermia since they can be treated noninvasively via surface irradiation [Zhao 2011].

Heat therapy has been used for twenty years and has been shown to result in local control for a number of tumor types [Zhao 2011]. Hyperthermia has been used alone and in combination with other treatments [Dereski 1995]. Hyperthermia-induced cytotoxicity depends on both temperature and heating time. Hyperthermia occurs at temperatures between 40 and 44˚C, which is cytotoxic for tumor cells due to insufficient blood perfusion via the tumor vasculature [Van der Zee 2002]. For optimum effect, the elevated temperatures are typically maintained over a period ranging from 30 to 60 min. Due to impaired blood flow, tumors have reduced thermoregulatory abilities resulting in preferential heating during hyperthermia. Furthermore, reduced blood flow results in deprivation of oxygen and nutrients to tumors making them more heat sensitive [Field 1979]. Hyperthermia is a strong sensitizer of radiotherapy and a number of cytotoxic drugs: combination therapies consisting of hyperthermia and radiotherapy or chemotherapy have been shown to produce additive effects, as long as the treatments are administered without a significant time gap. Hyperthermia likely enhances the effects of chemotherapy by increasing tumor perfusion resulting in increased drug delivery [Van der Zee 2002].

The limiting factor in chemotherapeutic treatment regimens is drug toxicity. Previous experiments with murine tumors have shown positive results by using radiation,

chemotherapy, and hyperthermia in different combinations. For example, hyperthermia in combination with bleomycin increased cell death and tumor regression [Rao 2010]. The chemotherapy-hyperthermia combination has also shown improvement of survival rates and quality of life in patients [Zhao 2011]. Previous studies have shown that exposing cells to high temperatures can alter the fluidity of the cellular membrane and inhibit protein synthesis. Hyperthermia can also destroy enzymes involved in DNA synthesis and cause cytotoxic effects. These effects can lead to structural alterations in biological macromolecules, increase oxygen concentrations in the cell, affect material transport, and alter energy conversion. Many studies have also shown that hyperthermia leads to apoptosis [Zhao 2011].

PDT has been used in combination with hyperthermia both *in vivo* and *in vitro*. For example, Dereski et al (1995) found that the effects were greater than additive when hyperthermia was given post-PDT. Hyperthermic temperatures were found to inhibit repair of sub-lethal damage thereby making hypoxic cells more sensitive to PDT. Using a murine mammary adenocarcinoma model, Chen et al (1996) showed that the combination of PDT and hyperthermia produced a synergetic tumor response. Hirschberg et al, (2004) examined synergistic effects of 5-aminolevulinic acid-mediated PDT and hyperthermia concurrently on human and rat glioma spheroids. The results showed that, when administered separately, PDT and hyperthermia were not very effective, however, concurrent administration of the two treatment modalities resulted in significant toxicity.

1.7 Multicellular Tumor Spheroids

A spheroid is an *in vitro* tumor model that has some characteristics of *in vivo* tumors [Dubessy 2000]. Multicellular tumor spheroids (MCTS) are three-dimensional collection of cells that mimic small tumors and metastases. MCTS have cellular heterogeneity which is a property of most solid tumors [Mueller-Klieser 2000]. The biological behavior of spheroids and their shape are similar to tumor nodules and they are therefore more representative of an *in vivo* situation than monolayer cell cultures. MCTS represent an excellent model for the initial evaluation of experimental therapies [Hirschberg 2004].

Spheroids are formed from the aggregation of multiple clonogenic cells. The cells proliferate exponentially and are weakly bound together. After a few hours, a critical cell density is reached and the spheroid becomes reinforced by intercellular links such as gap junctions and desmosomes [Dubessy 2000].
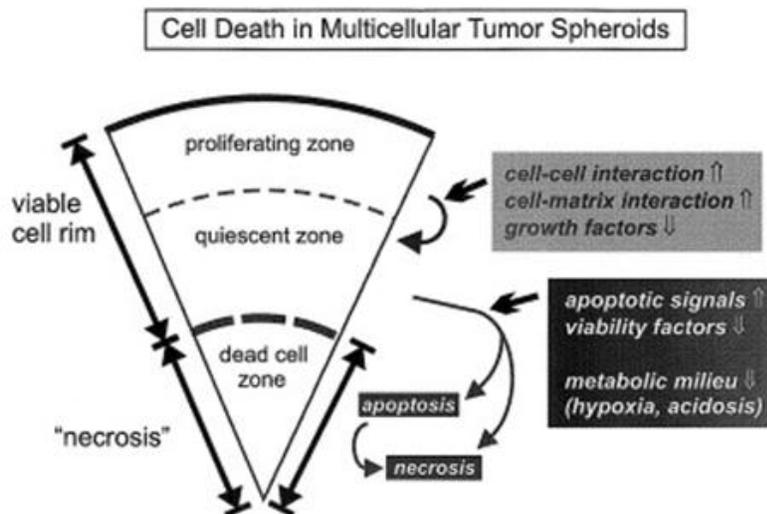

Figure 9. The pathway spheroids undergo when cells move from the viable outer surface to the necrotic center and cell death [Mueller-Klieser 2000].

As illustrated in Figure 9, cells are stratified into three layers according to oxygen, pH and nutrient gradients: an outer proliferative layer that is in contact with a nutrient-rich medium, a non-proliferative layer lacking in oxygen and nutrients and a necrotic core consisting of dead cells. Due to the limited diffusion of oxygen and nutrients, a necrotic core develops when the spheroid reaches a diameter of 200-500 μm. [Dubessy 2000]. Since MCTS are cultured from genetically stable cell lines, the structure can be reproduced. This allows for reproducibility of growth kinetics, diameter of the necrotic center, and viable rim of cells over multiple experiments. The necrotic core typically grows at a similar rate as the viable outer surface [Mueller-Klieser 2000]. The size of necrosis varies by spheroid diameter, cell line, oxygen gradient, pH, and nutrients [Dubessy 2000]. Spheroid viability can be determined by measuring its volume or by measuring the necrotic center or viable rim thickness.

The ability of spheroids to mimic oxygen gradients found in tumor nodules *in vivo* makes them ideally suited for investigational studies involving oxygen-dependent therapies such as PDT and ionizing radiation. In this respect, the non-proliferating quiescent cells in hypoxic regions of spheroids are particularly relevant since they represent a cell population resistant to oxygen-dependent therapies. The efficacy of a therapy is critically dependent on its ability to eradicate these cells. The primary disadvantage of MCTS is their inability to model tumor vasculature. Additionally, MCTS lack the cellular heterogeneity of tumors *in vivo* as well as a functioning immune system [Madsen 2006].

Not surprisingly, studies show that MCTS are less sensitive to PDT than monolayers. As the size of the spheroid increases, the sensitivity to PDT decreases.

These observations can be explained in terms of oxygen availability. For example, cells in monolayers are well oxygenated whereas a significant fraction of cells in spheroids are located in hypoxic areas and therefore exhibit an increased resistance to oxygen-mediated therapies such as PDT. Uneven photosensitizer distributions in spheroids are also a contributing factor to their increased PDT resistance compared to monolayers [Dubessy 2000].

1.8 Scope of Study

The overall objective of the proposed work is to determine whether hyperthermia increases the efficacy of PCI-mediated delivery of bleomycin in an *in vitro* model consisting of human glioma spheroids. It is hypothesized that PCI, performed under hyperthermic conditions, will increase the efficacy of bleomycin as determined from spheroid survival and growth kinetics. Furthermore, it is hypothesized that, under appropriate light irradiation and temperature levels, the interaction between PCI and hyperthermia is synergistic rather than additive.

CHAPTER 2

MATERIALS AND METHODS

2.1 Cell Line

All cell line manipulations were performed in a Labconco Purifier Class A2 Biological Safety Cabinet at the University of Nevada, Las Vegas. The human glioma cell line (ACBT; University of California, Irvine) was obtained from biopsy. Cells were incubated at 37°C, 5.0% CO_2, and 95% humidity inside a Shell Lab CO_2 Series incubator. The cell line was kept in Gibco Dulbecco's Modified Eagle Medium (DMEM) High Glucose 1X with 10% heat-inactivated fetal bovine serum (FBS), 25mM HEPES buffer (pH 7.4), penicillin (100U/ml), and streptomycin (100 μg/mL). The monolayer cells were passed twice a week using the same procedure. The confluency of the flask was noted prior to washing with 5mL of Gibco phosphate buffered saline (PBS) with pH of 7.2 and emptied of any remaining media. Next, 1 mL of Gibco 0.25% Trypsin-EDTA was added to the flask and left to sit for 5 minutes. Trypsin is a proteolytic enzyme that allows the ACBT cells to detach from the bottom of the flask. After 5 minutes, the flask was tapped against the lab cabinet to help detach any cells remaining in the flask. Then, 4 mL of DMEM was added to the flask and pipetted up and down and transferred to a 15 mL centrifuge tube. In order to maintain the cell line, 500 uL was added to 4.5 mL of DMEM in a new flask and the whole process was repeated.

2.2 Spheroid formation

Spheroids were formed using a modified centrifugation method first described by Ivascu and Kubbies [2006]. Briefly, 5,000 ACBT cells were detached from the growth flask; the exact number of cells was determined from coulter counting. The cells were pipetted into one well of a 96-well plate. Each round bottomed well was coated with matrigel and the plate was centrifuged at 1000g for 10 min. Following centrifugation, the well plate was placed in a CO_2 incubator for 48 h to allow them to take on the usual 3-dimensional spheroid morphology.

2.3 PDT and PCI treatments

After 48 hours, the resultant 350-400 μm diameter spheroids were transferred from the 96-well plate to 35 mm irradiation dishes where they were incubated in 1 μg/mL $AlPcS_{2a}$ for 18 h at 37 ^oC and 5% CO_2. Following incubation, spheroids were washed and placed into new medium. Spheroids in the PCI group were then subjected to an additional incubation in 0.25 μg/mL of bleomycin for 4 h. Following incubation, spheroids in both PDT and PCI groups were irradiated with a photodiode laser (wavelength = 670 nm) coupled to a 200 μm diameter optical fiber fitted with a micro-lens. In all cases, spheroids were subjected to an irradiance of 5 mW cm^{-2} for a range of times required to deliver radiant exposures ranging from 0.5 to 3.0 J cm^{-2}. All irradiations were performed at 37 ^oC in a temperature controlled incubator. This was accomplished by inserting the laser-coupled optical fiber through a small aperture located at the top of the incubator.

Following light exposure, 16 spheroids from each dish were placed into separate wells of an agarose coated Costar 48-well plate containing 750 μL of DMEM. Spheroid growth kinetics were monitored by recording two orthogonal diameters of each spheroid using a microscope with a calibrated eyepiece micrometer. Spheroid growth was measured 24 h after treatment and then twice a week over a 29-day period. After each measurement, 400 μL of DMEM was removed and replaced with 400 μl of fresh DMEM to provide the spheroids with adequate nutrients.

2.4 Hyperthermia

The 35 mm dishes containing medium and spheroids were placed in a temperature controlled incubator for 40-50 min. at temperatures ranging from 40° to 50° C. In the case of the combined treatments (PDT + HT; PCI + HT), spheroids were placed in the incubator 40 min. prior to light irradiation. Irradiances and radiant exposures were identical to those described previously. Following treatment, spheroids were placed in a 48-well plate and monitored as previously described. In all cases, the temperature of the incubator was monitored using a standard laboratory thermometer.

2.5 Statistical Analysis

All data were analyzed and graphed using Microsoft Excel. The two orthogonal diameter averages were used to calculate the average diameter of the spheroids. Each experiment included around 16 spheroids per group and was repeated 2-3 times and the average volume was calculated ($V = 4/3\ \pi r^3$). Standard errors were used throughout to calculate the error bars.

The degree of interaction between PCI and hyperthermia was evaluated according to the method of Drewinko et al. (1976). In this scheme the degree of interaction is given by

$$\alpha = \frac{SF^{PCI} \; x \; SF^{HT}}{SF^{PCI+HT}} \tag{1}$$

where SF^{PCI} and SF^{HT} represent the surviving fractions following PCI and hyperthermia, respectively, and SF^{PCI+HT} is the surviving fraction after combined treatments. In this analysis, $\alpha = 1$ indicates an additive effect (or absence of any effect), $\alpha > 1$ indicates a synergistic effect and $\alpha < 1$ indicates an antagonistic effect.

CHAPTER 3

RESULTS

3.1   Radiant exposure of 0.5 J cm^{-2}

3.1.1   37°C and 50°C

Based on results from previous *in vitro* PCI studies, an initial radiant exposure of 0.5 J cm^{-2} was chosen. The purpose of the initial set of experiments was to: (1) evaluate the efficacy of very low light exposures, and (2) determine the hyperthermic threshold for this particular *in vitro* model. In order to avoid data clutter, the three control curves at physiological temperature have been plotted in Figure 10. The control groups show similar growth kinetics over the 29-day observation period. At the time of irradiation (day 0), spheroid diameters ranged from 350-400 μm. ACBT spheroids typically reach a growth plateau at diameters ranging from 1100-1500 μm which, in these studies, occurred approximately four weeks following irradiation, thus providing the rationale for the 29-day observation period.
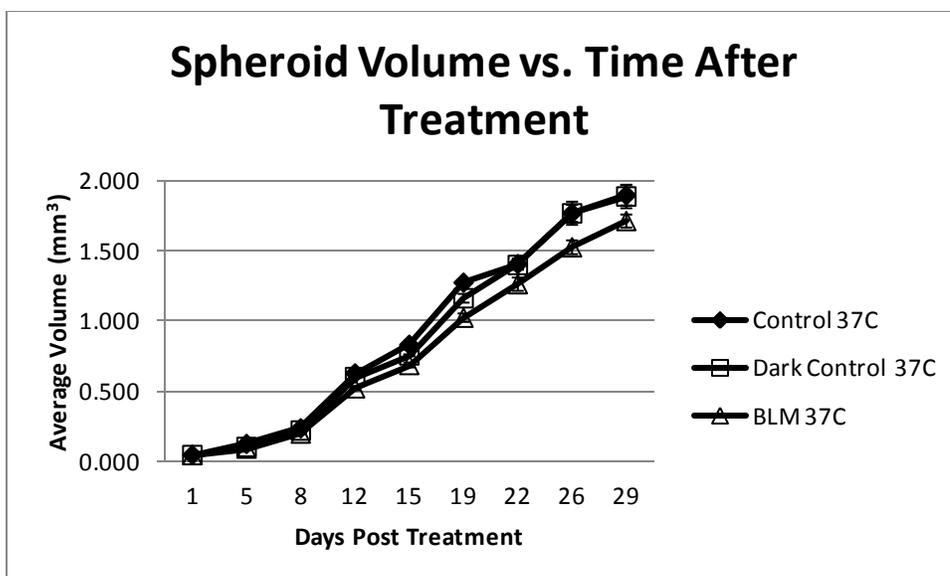
Figure 10. Average spheroid volume over a 29-day period at 37˚C for control groups. The true control group (no treatment) is denoted by Control, while Dark Control and BLM represent spheroids incubated in 1 μg ml^{-1} AlPcS$_{2a}$ and 0.25 μg ml^{-1} BLM, respectively.

The data in Figure 11 show complete growth inhibition of all spheroids (control and treatment groups) subjected to 50 ^{o}C for 50 min. Clearly, lower temperatures must be chosen. No significant differences in growth kinetics between the PCI and PDT groups were observed at 37 ^{o}C suggesting that a radiant exposure of 0.5 J cm^{-2} was too low.
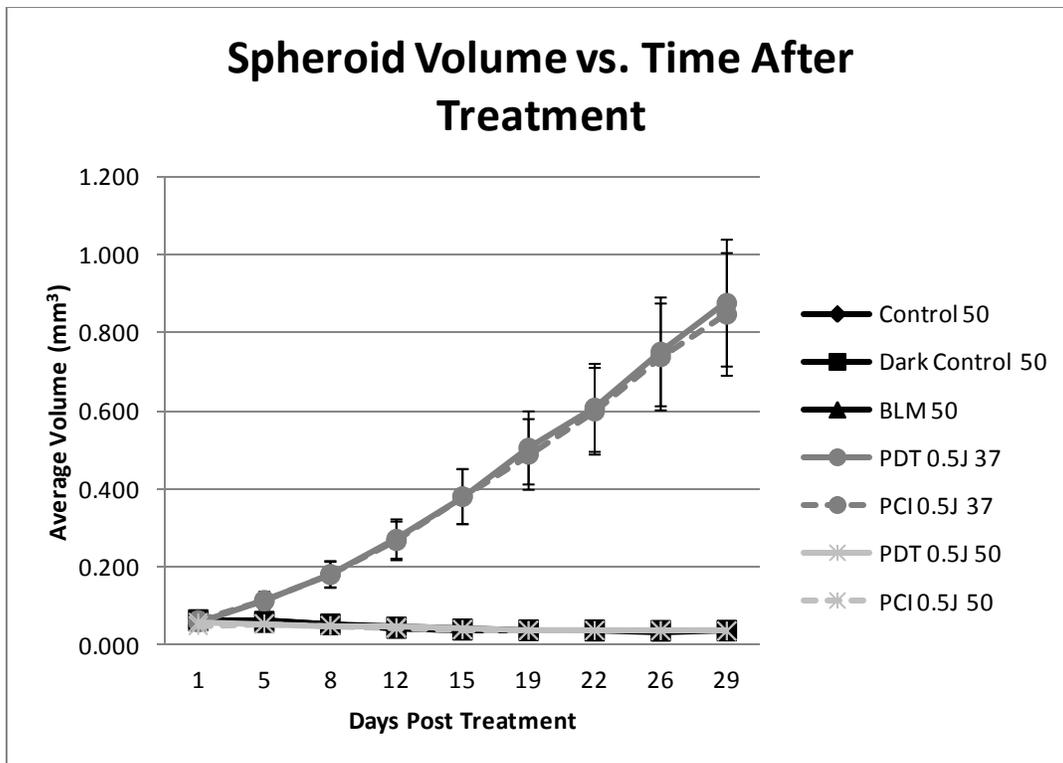
Figure 11. Average spheroid volume over a 29-day period at 37and 50˚C.

3.1.2   40°C and 45°C
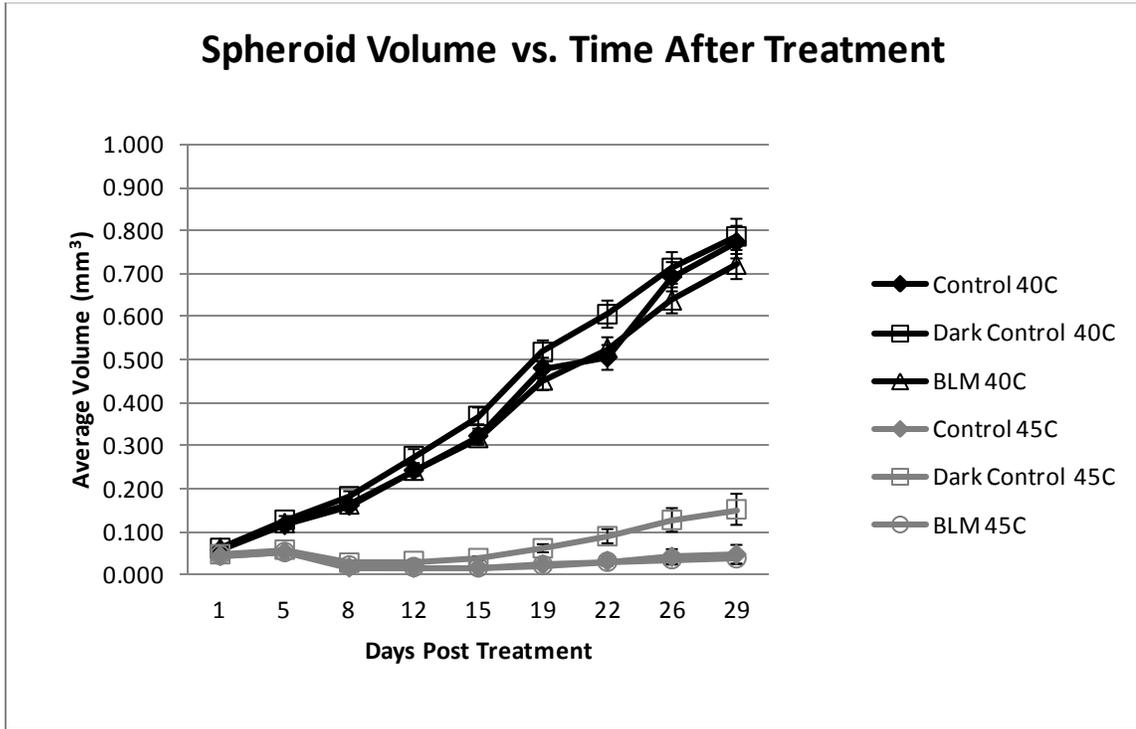
Figure 12. Average spheroid volume over a 29-day period for control groups at 40 and 45°C.

At temperatures of 45°C, all controls showed significant growth inhibition compared to spheroids subjected to 40°C (Figure 12). These results suggest that the threshold for complete heat-induced cell death occurs somewhere between 40 and 45°C. As illustrated in Figure 13, no significant differences were observed between the PDT and PCI groups at 40 °C suggesting that a higher radiant exposure is required. Not surprisingly, high temperature PDT and PCI resulted in complete growth inhibition.
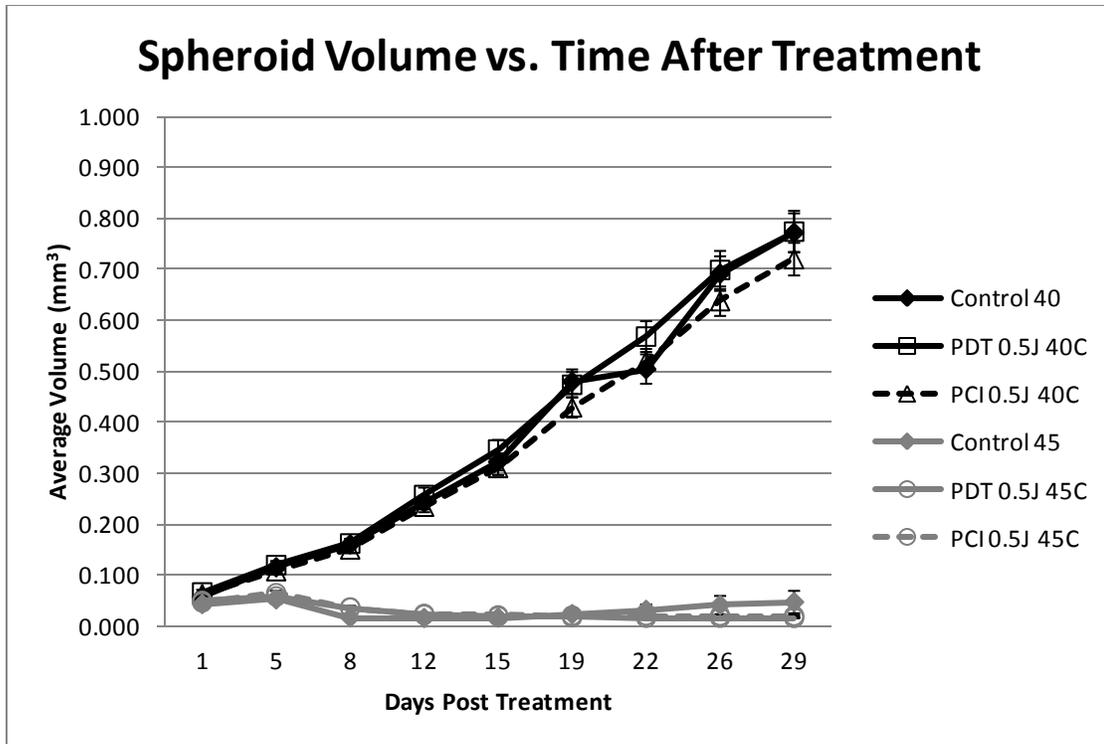
Figure 13. Average spheroid volume over a 29-day period at 40˚C and 45˚C.

3.1.3   42˚C

The data in Figure 14 show that spheroids in both treatment and control groups were growing throughout the observation period. No significant growth differences were observed between spheroids in the two treatment groups and between spheroids in the control and treatment groups. Again, this is highly suggestive of inadequate light exposure levels. The data in Figures 12-14 show that the threshold for complete heat-induced cell death occurs somewhere between 42 and 45°C. For this reason, a temperature of 42°C was chosen for the majority of studies presented in this work.
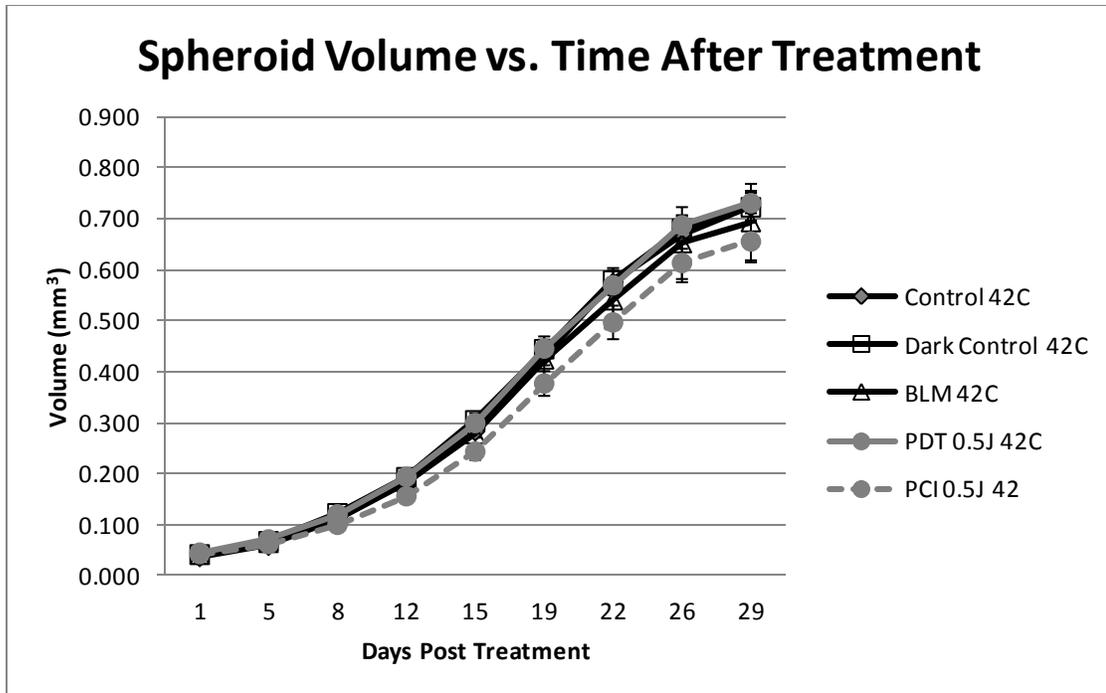
Figure 14. Average spheroid volume over a 29-day period at 42˚C.

3.2 Radiant exposure of 1.0 J cm^{-2}
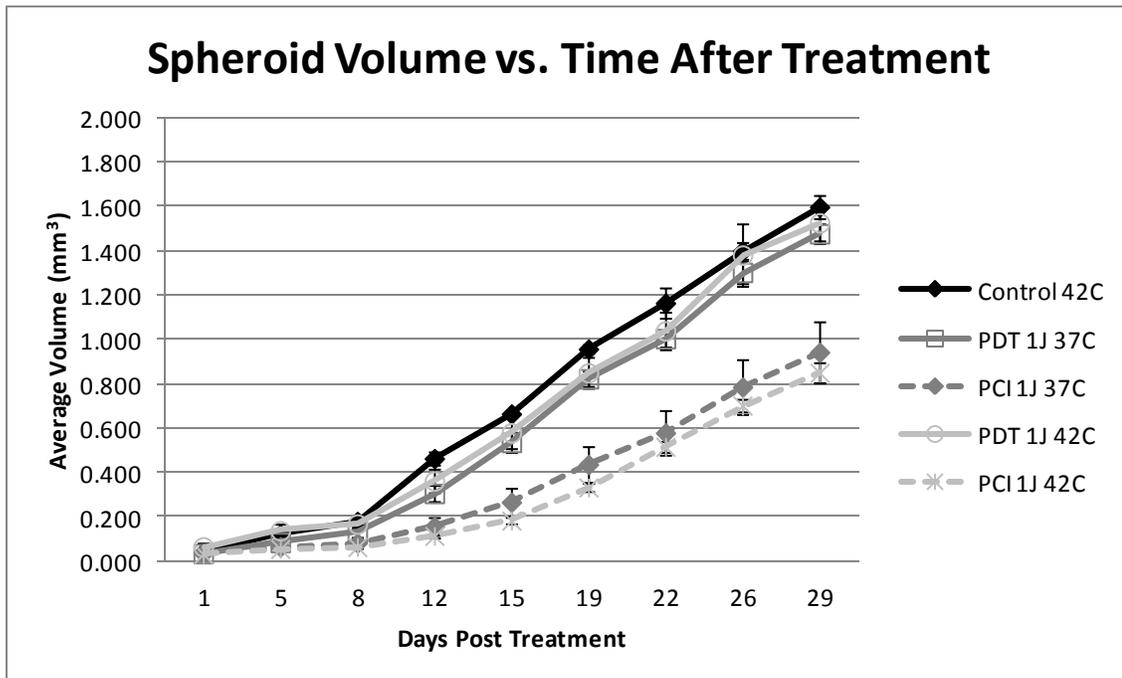
Figure 15. Average spheroid volume over a 29-day period for 1J cm^{-2} at 37˚C and 42˚C.

As shown in Figure 15, radiant exposures of 1.0 J cm^{-2} failed to produce significant differences in the growth kinetics of spheroids subjected to PCI at the two temperatures investigated. Even at this low light level, significant growth differences were observed between PCI- and PDT-treated spheroids at both temperatures. This suggests that the observed effect is not attributable to PDT.

3.3 Radiant exposure of 1.5 J cm^{-2}

PCI and PDT at 40 $^{\circ}$C resulted in a statistically significant reduction in survival compared to controls (Figure 16). At 37 $^{\circ}$C, neither treatment was effective, resulting in 100% survival (data not shown). The alpha coefficient (from equation 1) was found to be 1.4 suggesting a relatively low degree of synergism between 1.5 J PCI and 40 $^{\circ}$C.
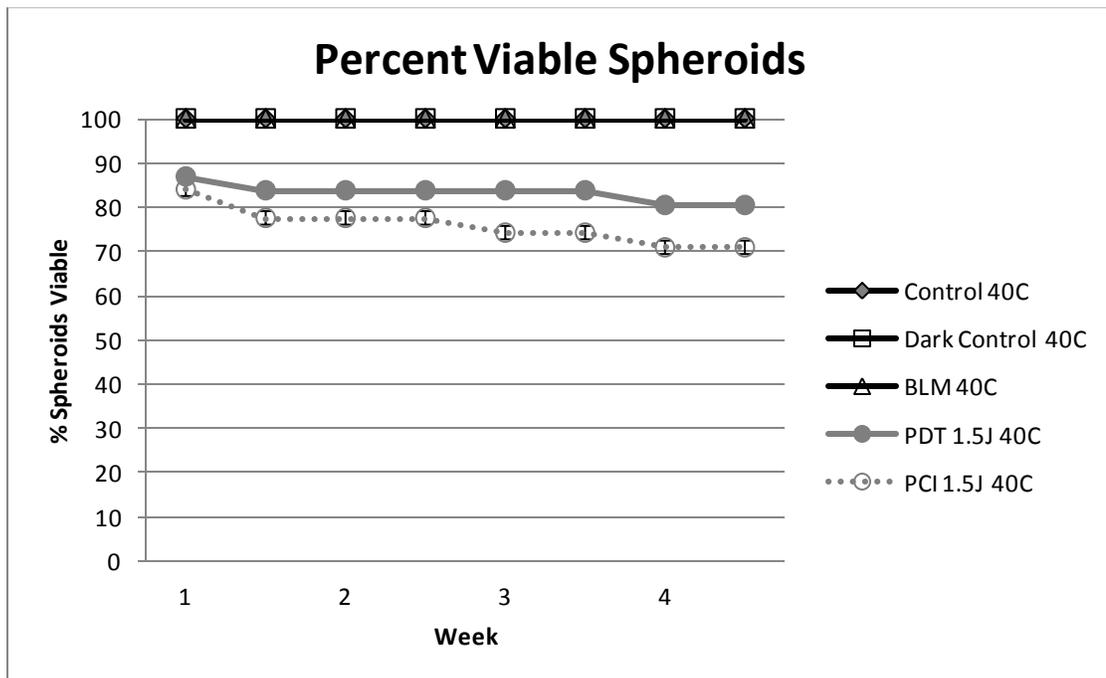
Figure 16. The percentage of viable spheroids over a four-week period at 40˚C.
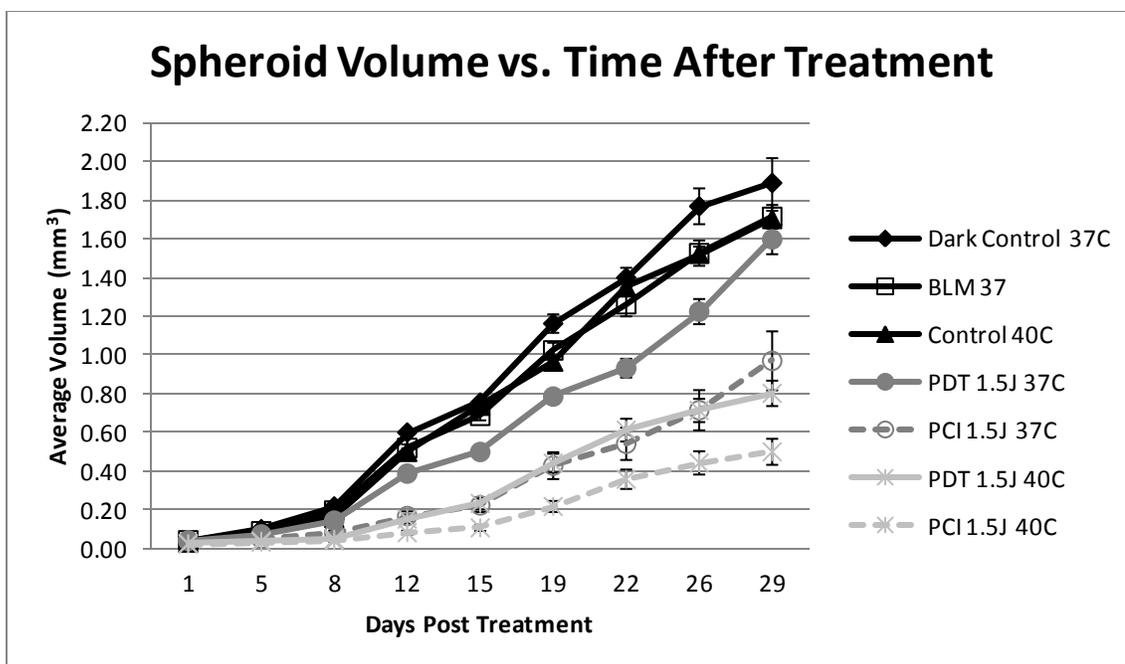
Figure 17. Average spheroid volume over a 29-day period at 1.5 J cm^{-2} for 37 and 40˚C.

The data in Figure 17 show that PDT and PCI at 1.5 J cm^{-2} were more effective than treatments at the lower light levels. For both temperatures investigated, PCI induced greater growth inhibition than PDT. Both PDT and PCI were more effective at the higher temperature thus illustrating the therapeutic advantage conferred by hyperthermia. The effectiveness of combined PCI and hyperthermia at 1.5 J cm^{-2} can be appreciated by comparing the final spheroid volume (ca. 0.5 mm^3) to the final volume obtained for the combined treatments at 1.0 J cm^{-2} (ca. 0.8 mm^3: Figure 15).

3.4 Radiant exposure of 2.5 J cm^{-2}
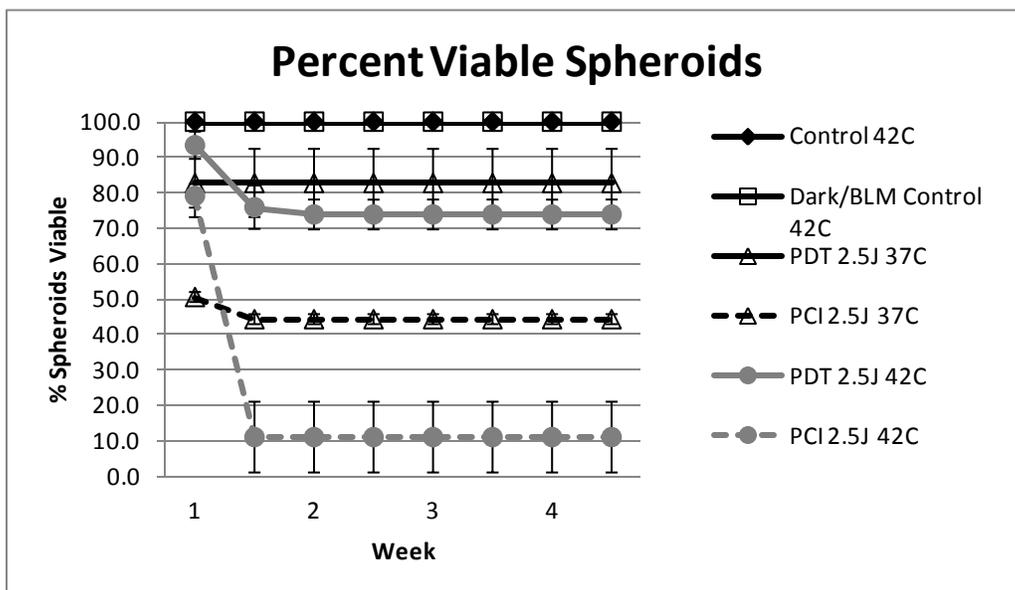
Figure 18. The percentage of viable spheroids over four weeks for 37˚C and 42˚C at 2.5 J cm^{-2}. The Dark/BLM Control group represents spheroids incubated in AlPcS$_{2a}$ for 18 h followed by a 4 h incubation in bleomycin (no light treatment).

PDT and PCI treatments at a radiant exposure of 2.5 J cm^{-2} resulted in spheroid toxicity significantly higher than observed at the lower light levels. This was particularly the case for the PCI treatments where survivals of approximately 43 and 10 % were observed at temperatures of 37 and 42°C, respectively (Figure 18). The α coefficient (4.3) suggests a significant degree of synergism between PCI and hyperthermia (42 ^{o}C) at this radiant exposure. The enhanced efficacy at 2.5 J cm^{-2} is also evident from the growth kinetics data in Figures 19 and 20. Of particular relevance is the combined PCI – hyperthermia data in Figure 20 showing almost complete spheroid growth inhibition as evidenced from the mean spheroid volume at the end of the observation period (0.2 mm^{3}).
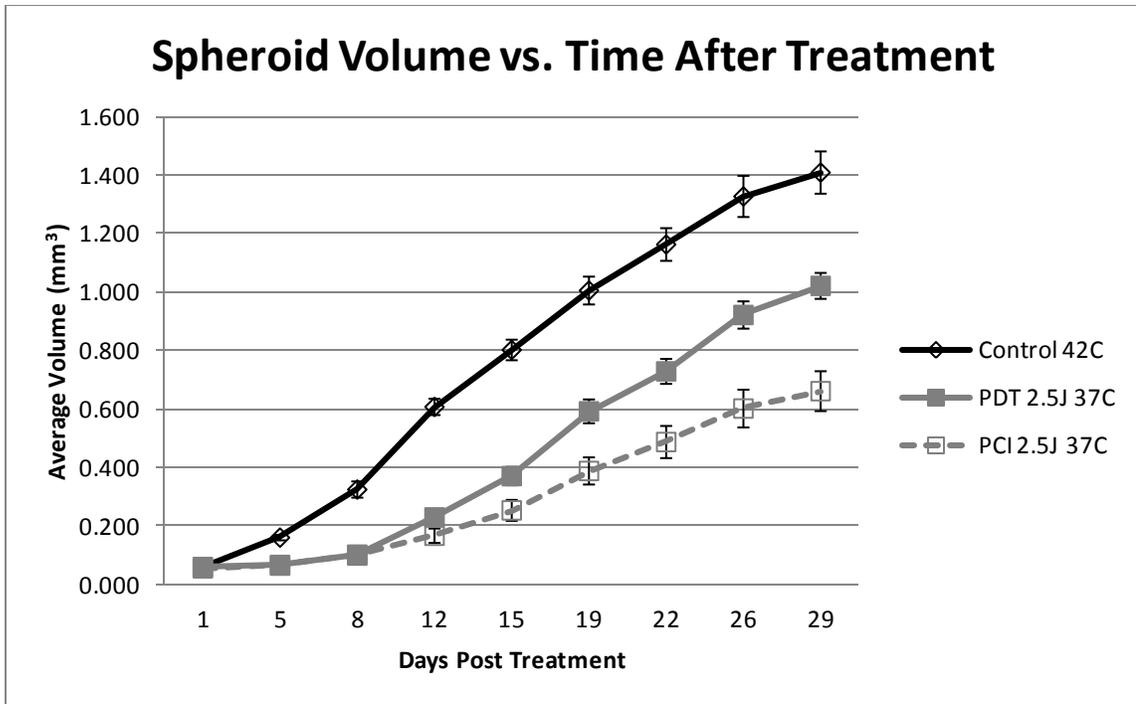
Figure 19. Average spheroid volume over a 29 day period for 37˚C at 2.5J cm^{-2}.
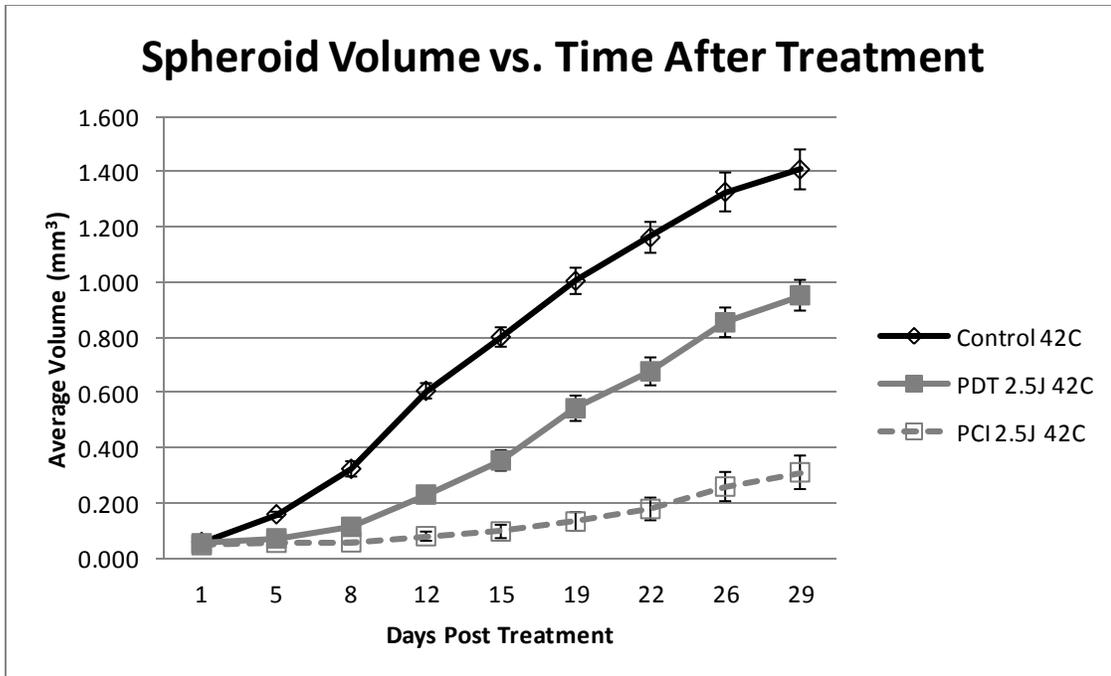
Figure 20. Average spheroid volume over a 29-day period for 42 ˚C at 2.5 J cm^{-2}.

3.5 Radiant exposure of 3 J cm^{-2}

Complete growth inhibition was observed in all treatment groups, even at physiological temperatures (37°C; Figure 21). The data suggest that this light level was too high.
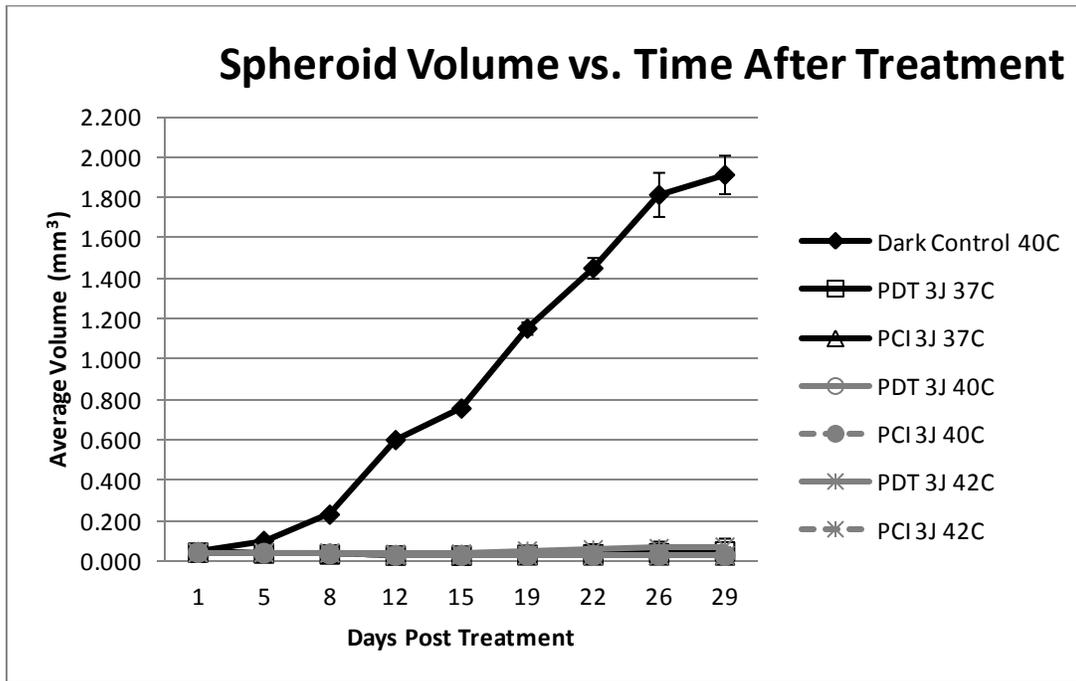
Figure 21. Average spheroid volume over a 29-day period for 37, 40 and 42 $^{\circ}$C at 3J cm^{-2}.

CHAPTER 4

DISCUSSION

PCI is a specialized application of PDT that may be used to enhance the delivery of macromolecules including chemotherapeutic agents such as bleomycin. This therapeutic modality is appealing for a number of reasons including: (1) the lack of size restrictions on the therapeutic molecules to be delivered, (2) high site specificity which confines the biological effect to light-illuminated volumes thus minimizing side effects of the drug, (3) increased therapeutic efficacy of a wide range of macromolecules allowing for the possibility of lower drug doses resulting in decreased morbidity, (4) high suitability for combination with other strategies for targeted drug delivery, thereby increasing the potential for further therapeutic improvements [Berg 1999; Dietze 2005; Selbo 2001; Selbo 2010; Weyergang 2011].

Although PCI has been investigated in a variety of cancer models, the particular emphasis of this thesis was the treatment of high grade gliomas such as GBM. These tumors pose a significant therapeutic challenge: due to their diffuse and infiltrative nature, complete surgical resection is virtually impossible. The propensity of glioma cells to migrate along white matter tracts suggests that a cure is possible only if these migratory cells can be eradicated. The observation that 80% of GBMs recur within 2 cm of the resection cavity [Wallner 1989] suggests that the development of local therapies may prove to be an effective strategy for the eradication of glioma cells in the resection margin, or brain-adjacent-to-tumor (BAT). Unfortunately, the delivery of therapeutic

agents to the BAT is complicated by variations in the patency of the BBB which is leaky in some regions and intact in others [Madsen 2010]. The BBB controls the passage of blood-borne agents into the central nervous system and, as such, it plays a vital role in protecting the brain against pathogens. Although this protective mechanism is essential for normal brain function, it also poses a significant hindrance to the entry of drugs into the brain. The protective function of the BBB is especially problematic for the treatment of infiltrating gliomas. Although surgery is used to remove gross tumor, standard adjuvant therapies consisting of radiation and chemotherapy have proven inadequate for eradicating infiltrating cells in the BAT. In the case of chemotherapeutic drugs, this is due to their inability to penetrate the intact BBB. Therefore, elimination of glioma cells in the BAT is unlikely to be accomplished until methods are developed to: (1) deliver drugs or carriers across the BBB at selected sites, or (2) selectively disrupt the BBB [Madsen 2010].

Selective disruption of the BBB by either PDT or PCI may prove useful for enhancing the delivery of therapeutic agents for the treatment of a variety of brain diseases including cancer. Localized opening of the BBB has been accomplished using a number of techniques including ultrasound [Vykhodtseva 2008] and laser-based approaches such as PDT [Hirschberg 2008] and PCI [Hirschberg 2009]. These methods are appealing due to the highly localized nature of the BBB disruption: in contrast to the use of hyperosmolar solutions, the BBB is only disrupted at sites subjected to sufficient laser power densities which can be controlled by the user to coincide with the location of the pathology. Through careful choice of beam parameters, the targeted volume can be as small as a few mm^3. Of particular interest are observations showing that these highly

focused approaches do not cause permanent damage to the BBB, as long as incident power densities remain below threshold levels [Hirschberg 2009]. Under these conditions, the BBB may remain open for relatively long periods of time thus facilitating multi-fractionated drug delivery.

Selective disruption of the BBB via PCI-mediated delivery of *Clostridium perfringens* epsilon prototoxin (Clp) was recently demonstrated in Fischer rats [Hirschberg 2009]. Clp was chosen due to the ability of active toxin to cause widespread and reversible opening of the BBB [Worthington 1975; Nagahama 1991; J. Dorca-Arevalo 2008]. Following systemic administration, Clp prototoxin is converted to active toxin via proteolytic cleavage. The results demonstrated that Clp-PCI was capable of causing localized BBB disruption at very low light fluences (1 J). Based on magnetic resonance images, maximum BBB opening occurred 3 days following PCI and pathology analyses revealed no permanent BBB damage at these low light levels.

In a follow-on study, using an orthotopic brain tumor model consisting of F98 glioma cells in Fischer rats, newly implanted tumor cells were used to mimic the characteristics of infiltrating cells in the resection margin usually found following surgical removal of gross tumor [Madsen 2006]. PDT- or PCI-localized BBB opening was performed 24 h following cell inoculation. This is an insufficient time to allow for the development of bulk tumor and BBB degradation, but long enough for the cells (doubling time of approximately 18 h) to form small, sequestered, micro-clusters which are protected by an intact BBB. The survival of animals implanted with F98 tumor cells was significantly extended following BLM chemotherapy with PCI-mediated BBB opening compared to controls that received chemotherapy only.

As has been shown, the BBB presents a significant obstacle to the delivery of chemotherapeutic agents, such as bleomycin, to glioma cells residing in the BAT. Endosomal entrapment is another factor limiting the efficacy of bleomycin and it was this problem that was addressed in this thesis. PCI-mediated delivery of bleomycin has been investigated in glioma spheroids [Mathews (in press)] and the results are in qualitative agreement with the findings of this work, i.e., at sufficient radiant exposures (1.5 J cm^{-2}) PCI enhances the efficacy of bleomycin as demonstrated by decreased spheroid survival and reduced growth kinetics compared to PDT controls. In the previous study, PCI was examined at relatively low light levels ($\leq$ 1.5 J cm^{-2}) and all studies were performed at physiological temperatures (37°C). The studies performed in this thesis extend the previous work by examining the effects of higher light doses and, most importantly, the combination of PCI and hyperthermia.

The exact hyperthermic threshold, i.e., the temperature resulting in a significant diminution in spheroid survival was somewhat difficult to ascertain due to inaccuracies in the thermoregulatory capabilities of the incubator in which the cells were irradiated. Based on temperature readings during the exposures, the incubator was deemed accurate to 1.0 degrees C. Based on the data presented in Figures 12 and 14 all control spheroids were viable at 42 $^{\circ}$C while almost all were dead at 45 $^{\circ}$C thus suggesting a threshold close to 45°. This is in qualitative agreement with the results of Hirschberg et al. [Hirschberg 2004] who observed significant hyperthermia-induced glioma spheroid death at temperatures between 46 and 49°C. The slight differences between experiments may be due to differences in spheroid formation techniques (agar overlay method vs. centrifugation) which produce slight variations in spheroid morphology. From the results

presented in Figs. 12 and 14, it was decided to use a temperature of $42^{\circ}C$ for the majority of studies. This has significant clinical relevance since many patients undergoing hyperthermia or combined hyperthermia therapies are treated at this temperature. In future studies, the use of calibrated thermocouples immersed directly in the cell medium would be a more accurate method of determining the temperature compared to the technique used in the present work, i.e., the measurement of air temperature using thermometers.

Of particular relevance are the results showing that hyperthermia can enhance the effects of PCI-mediated delivery of bleomycin (Figs. 16-18, 20). The degree of interaction between the two modalities was found to be critically dependent on light dose: no effect was observed at radiant exposures below 1.5 J cm^{-2}, while low and high degrees of synergism were observed at 1.5 and 2.5 J cm^{-2}, respectively. This is the first observation of a synergistic interaction between PCI and hyperthermia.

Although the mechanism of synergism between PCI and hyperthermia is unknown, it likely has several components. For instance, it might be due, in part, to thermally-induced inhibition of DNA repair enzymes [Van der Zee 2002]. Bleomycin produces DNA damage and this damage is likely exacerbated if the function of repair enzymes is inhibited by hyperthermia. Additionally, hyperthermia is known to cause damage to cellular membranes [Silva 2011] and, by implication, to endosomal membranes. Subsequently, these heat-damaged membranes may be more susceptible to the effects of PCI resulting in an enhanced release of bleomycin.

CHAPTER 5

CONCLUSIONS

The overall objective of the proposed work was to determine whether hyperthermia increases the efficacy of PCI-mediated delivery of bleomycin in an *in vitro* model consisting of human glioma spheroids. The results show that hyperthermia and PCI interact in a synergistic manner over a very narrow range of light and temperature levels. A temperature of 45 $^{\circ}$C resulted in total spheroid death, while all spheroids subjected to 42 $^{\circ}$C survived. Therefore, the hyperthermic threshold was estimated to be between 42 and 45 $^{\circ}$C. This provided the rationale for the temperature range investigated (40 – 42 $^{\circ}$C). No significant differences in growth kinetics and survival were observed between PCI- and PDT -exposed spheroids at radiant exposures < 1.5 J cm^{-2}. In contrast, all PDT and PCI spheroids irradiated with 3.0 J cm^{-2} died, suggesting that the useful light range is between 1.5 and 3.0 J cm^{-2}.

The experiments show that hyperthermia enhanced the PCI-mediated delivery of bleomycin. A relatively low degree of synergism (α=1.4) was observed between PCI and hyperthermia at 1.5 J cm^{-2} and 40 $^{\circ}$C, while a high degree of synergism (α=4.3) was found when the two modalities were combined at a light level of 2.5 J cm^{-2} and a temperature of 42 $^{\circ}$C. This represents the first observation of a synergistic interaction between PCI and hyperthermia.

Future experiments should consider a better temperature monitoring technique. By using a thermocouple immersed directly in the cell solution, the temperature can be

monitored more accurately. Additional experiments might also examine radiant exposures of 2 J cm^{-2} to determine if the radiant exposure can be limited further to spare as many healthy cells as possible. Overall, the results provide the basis for additional *in vivo* experiments which could be performed using well established orthotopic rat brain tumor models.

Other experiments should examine the mechanisms underlying the observed synergism between the two treatment modalities. One possibility is that hyperthermia inhibits DNA repair enzymes. It was also postulated that hyperthermia can cause damage to cellular or endosomal membranes, thus resulting in an enhanced release of bleomycin in PCI. This could be examined by measuring intracellular concentrations of bleomycin as a function of temperature. Valuable insight into the mechanisms of synergism might be gained from studying the mode of cell death (apoptosis vs. necrosis) following combined treatments. Such studies would be relatively straightforward in the human glioma spheroid model used in this work.

Finally, the efficacy of hyperthermia and PCI should be investigated in different types of cancer cell lines in order to determine the overall utility of this combination therapy. A logical starting point would be to use spheroids since they can be formed from a wide range of cancer cells.

APPENDIX

LIST OF EQUATIONS

REFERENCES

Ambroz M, MacRobert AJ, Morgan J, Rumbles G, Foley MS, Phillips D. Time-resolved fluorescence spectroscopy and intracellular imaging of disulphonated aluminum phthalocyanine. J Photochem Photobiol B. 22(2): 105-17; 1994.

Berg K, Selbo PK, Prasmickaite L, Tjelle TE, Sandvig K, Moan J, Gaudernack G, Fodstad O, Kjolsrud S, Anholt H, Rodal GH, Hogset A. Photochemical internalization: a novel technology for delivery of macromolecule into cytosol. Cancer Res. 59(6): 1180-3; 1999.

Berg K, Selbo PK, Weyergang A, Dietze A, Prasmickaite L, Bonsted A, Engesaeter BO, Angell-Petersen E, Warloe T, Frandsen N, Hogset A. Porphyrin-related photosensitizers for cancer imaging and therapeutic applications. J Microsc. 218(Pt.2): 133-47; 2005.

Berg K, Folini M, Prasmickaite L, Selbo PK, Bonsted A, Engesaeter BO, Zaffaroni N, Weyergang A, Dietze A, Maelandsmo GM, Wagner E, Norum OJ, Hogset A. Photochemical internalization: a new tool for drug delivery. Curr Pharm Biotechnol. 8(6): 362-72; 2007.

Bonneau S, Morliere P, Brault D. Dynamics of interactions of photosensitizers with lipoproteins and membrane-models: correlation with cellular incorporation and subcellular distribution. Biochem Pharmacol. 68(7):1443-52; 2004.

CBTRUS. Statistical Report: Primary Brain Tumors in the United States, 2004-2007. Published by the Central Brain Tumor Registry of the United States; 2011.

Chandana SR, Movva S, Arora M, Singh T. Primary brain tumors in adults. Am Fam Physician. 77(10): 1423-30; 2008.

Chen Q, Chen H, Shapiro H, Hetzel FW. Sequencing of combined hyperthermia and photodynamic therapy. Radiat Res. 146(3): 293-7; 1996.

Clarke J, Butowski N, Chang S. Recent advances in therapy for glioblastoma. Arch Neurol. 67(3): 279-83; 2010.

Dereski MO, Madigan L, Chopp M. The effect of hypothermia and hyperthermia on photodynamic therapy of normal brain. Neurosurgery. 36(1):141-5; 1995.

Dietze A, Peng A, Selbo PK, Kaalhus O, Muller C, Bown S, Berg K. Enhanced photodynamic destruction of a transplantable fibrosarcoma using photochemical internalization of gelonin. Br J Cancer. 92(11): 2004-2009; 2005.

Dorca-Arevalo J, Soler-Jover A, Givert M, Popoff MR, Martin-Satue M, Blasi J. Binding of epsilon-toxin from clostridium perfringens in the nervous system. Vet Microbiol. 131(1-2): 14-25; 2008.

Drewinko B, Loo TL, Brown B, Gottlieb JA, Freireich EJ. Combination chemotherapy in vitro with adriamycin. Observations of additive, antagonistic, and synergistic effects when used in two-drug combinations on cultured human lymphoma cells. Cancer Biochem Biophys. 1(4): 187-195; 1976.

Dubessy C, Merlin JM, Marchal C, Guillemin F. Spheroids in radiobiology and photodynamic therapy. Crit Rev Oncol Hematol. 36(2-3): 179-92; 2000.

Fadul CE, Wen PY, Kim L, Olson JJ. Cytotoxic chemotherapeutic management of newly diagnosed glioblastoma multiforme. J Neurooncol. 89(3): 339-57; 2008.

Field SB, Bleehen NM. Hyperthermia in the treatment of cancer. Cancer Treat Rev. 6(2): 63-94; 1979.

Gupta S, Dwarakanath BS, Muralidhar K, Koru-Sengul T, Jain V. Non-monotonic changes in clonogenic cell survival induced by disulphonated aluminum phthalocyanine photodynamic treatment in a human glioma cell line. J Transl Med. 8:43; 2010.

Hirschberg H, Sun CH, Tromberg BJ, Yeh AT, Madsen SJ. Enhanced cytotoxic effects of 5-aminolevulinic acid-mediated photodynamic therapy by concurrent hyperthermia in glioma spheroids. J Neurooncol. 70(3):289-99; 2004.

Hirschberg H, Uzal FA, Chighvinadze D, Zhang MJ, Peng Q, Madsen SJ. Disruption of the blood-brain barrier following ALA-mediated photodynamic therapy. Lasers Surg Med. 40(8): 535-42; 2008.

Hirschberg H, Zhang MJ, Gach HM, Uzal FA, Peng Q, Sun CH, Chighvinadze D, Madsen SJ. Targeted delivery of bleomycin to the brain using photo-chemical internalization of Clostridium perfringens epsilon prototoxin. J Neurooncol. 95(3): 317-29; 2009.

Hogset A, Prasmickaite L, Selbo PK, Hellum M, Engesaeter BO, Bonsted A, Berg K. Photochemical internalization in drug and gene delivery. Adv Drug Deliv Rev. 56(1):95-115; 2004.

Iacob G, Dinca EB. Current data and strategy in glioblastoma multiforme. J Med Life. 2(4): 386-393; 2009.

Ivascu, A., Kubbies, M. Rapid Generation of Single-Tumor Spheroids for High Throughput Cell Function and Toxicity Analysis. J Biomol Screen 11(8): 922-32; 2006.

Koukourakis GV, Kouloulias V, Zacharias G, Papadimitriou C, Pantelakos P, Maravelis G, Fotineas A, Beli I, Chaldeopoulos D, Kouvaris J. Temozolomide with radiation therapy in high grade brain gliomas: pharmaceuticals considerations and efficacy; a review article. Molecules. 14(4): 1561-77; 2009.

Linnert M, Gehl J. Bleomycin treatment of brain tumors: an evaluation. Anticancer Drugs. 20(3): 157-64; 2009.

Madsen SJ, Sun CH, Tromberg BJ, Cristini V, De Magalhaes N, Hirschberg H. Multicell tumor spheroids in photodynamic therapy. Lasers Surg Med. 38(5): 555-564; 2006.

Madsen SJ, Hirschberg H. Site-specific opening of the blood-brain barrier. J Biophotonics. 3(5-6): 356-67; 2010.

Mathews M, Angell-Petersen E, Sanchez R, Sun C, Vo V, Hirschberg H, Madsen S. The effects of ultra low fluence rate single and repetitive photodynamic therapy on glioma spheroids. Lasers Surg Med. 41(8): 578-584; 2009.

Mathews M, Blickenstaff JW, En-Chung Shih, Zamora G, Vo V, Hirschberg H, Madsen SJ. Photochemical internalization of bleomycin for glioma treatment: a new role for an old drug. Journal of Neuro-Oncology. (in press).

Mir LM, Tounekti O, Orlowski S. Bleomycin: revival of an old drug. Gen Pharmacol. 27(5):745-8; 1996.

Morrow T. Barrett's esophagus seen in new photodynamic light. Manag Care. 12(8): 44-45, 2003.

Mueller-Klieser W. Tumor biology and experimental therapeutics. Crit Rev Oncol Hematol. 36(2-3): 123-39; 2000.

Nagahama M, Sakurai J. Distribution of labeled clostridium perfringens epsilon toxin in mice. Toxicon. 29(2): 211-7; 1991.

Nishikawa R. Standard therapy for glioblastoma: a review of where we are. Neurol Med Chir (Tokyo). 50(9): 713-9; 2010.

Pan H, Alksne J, Mundt AJ, Murphy KT, Cornell M, Kesari S, Lawson JD. Med Oncol. November 23, 2011 [Epub ahead of print].

Peng Q, Moan J, Nesland JM, Rimington C. Aluminum phthalocyanines with asymmetrical lower sulfonation and with symmetrical higher sulfonation: a comparison of localizing and photosensitizing mechanism in human tumor LOX xenografts. Int J Cancer. 46(4): 719-26; 1990.

Pron G, Mahrour N, Orlowski S, Tounekti O, Poddevin B, Belehradek S, Mir LM. Internalization of the bleomycin molecules responsible for bleomycin toxicity: a receptor-mediated endocytosis mechanism. Biochem Pharmacol. 57(1): 45-56; 1999.

Rao W, Deng ZS, Liu J. A review of hyperthermia combined with radiotherapy/chemotherapy on malignant tumors. Crit Rev Biomed Eng. 38(1): 101-16; 2010.

Roy SN, Horwitz SB. Characterization of the association of radiolabeled bleomycin A2 with HeLa cells. Cancer Res. 44(4): 1541-6; 1984.

Selbo PK, Sivam G, Fodstad O, Sandvig K, Berg K. Photochemical internalization increases the cytotoxic effect of the immunotoxin MOC31-gelonin. Int J Cancer. 87(6): 853-859; 2000.

Selbo PK, Kaalhus O, Sivam G, Berg K. 5-Aminolevulinic acid-based photochemical internalization of the immunotoxin MOC31-gelonin generates synergistic cytotoxic effects in vitro. Photochem Photobiol. 74(2): 303-10; 2001.

Selbo PK, Weyergang A, Hogset A, Norum OJ, Berstad MB, Vikdal M, Berg K. Photochemical internalization provides time- and space-controlled endolysosomal escape of therapeutic molecules. J Control Release. 148(1): 2-12; 2010.

Silva AC, Oliveira TR, Mamani JB, Malheiros SM, Malavolta L, Pavon LF, Sibov TT, Amaro E, Tannus A, Vidoto EL, Martins MJ, Santos RS, Gamarra LF. Application of hyperthermia induced by superparamagnetic iron oxide nanoparticles in glioma treatment. Int J Nanomedicin. 6:591-603; 2011.

Stubbe J, Kozarich JW, Ajmera S, Wu JC, Worth L, Rabow LE. DNA degradation by bleomycin: evidence of 2'R-proton abstraction and for C-O bond cleavage accompanying base propenal. Biochemistry. 25(21): 6586-92; 1986.

Umezawa H, Maeda K, Takeuchi T, Okami Y. New antibiotics, bleomycin A and B. J Antibiot. 19 (5): 200-9; 1966.

Van der Zee J. Heating the patient: A promising approach? Ann Oncol. 13(8): 1173-1184; 2002.

Vykhodtseva N, McDannold N, Hynynen K. Progress and problems in the application of focused ultrasound for blood-brain barrier disruption. Ultrasonics. 48(4): 279-96; 2008.

Wallner KE, Galicich JH, Krol G, Arbit E, Malkin MG. Patterns of failure following treatment for glioblastoma multiforme and anaplastic astrocytoma. Int J Radiat Oncol Biol Phys. 16(6): 1405-9; 1989.

Weyergang A, Selo PK, Berstad ME, Bostad M, Berg K. Photochemical internalization of tumor-targeted protein toxins. Lasers Surg Med. 43(7): 721-33; 2011.

Worthington RW, Mulders MS. Effect of clostridium perfringens epsilon toxin on the blood brain barrier of mice. Onderstepoort J Vet Res. 42(1): 25-7; 1975.

Zaniboni A, Prabhu S, Audisio RA. Chemotherapy and anesthetic drugs: too little is known. Lancet Oncol. 6(3):176-181; 2005.

Zhao L, Ouyang W, Zhang Y, Liao Y, Tang J, Zhou J, Wang X, Du L. Effect of hyperthermia on the apoptosis and proliferation of CaSki cells. Mol Med Report. 4(1): 187-91; 2011.

Graduate College

University of Nevada, Las Vegas

Christina Schlazer

Local Address:
225 S Stephanie Street Apt. 324
Henderson NV 89012

Bachelor of Sciences in Physics
Binghamton University
2006

Bachelor of Arts in Mathematical Science
Binghamton University
2006

Dissertation/Thesis Title: Effects of Hyperthermia on Photochemical Internalization-Mediated Delivery of Bleomycin.

Dissertation/Thesis Examination Committee:

    Chairperson, Dr. Steen J. Madsen, Ph. D.

    Committee Member, Dr. Ralf Sudowe, Ph.D.

    Committee Member, Dr. Gary Cerefice, Ph.D.

    Graduate Faculty Representative, Dr. Janet Dufek, Ph.D.